ARMA 21–2015

Field Data Analysis and Modeling of Drillstring Vibrations to Identify Inefficiency in Deep Geothermal Drilling

Barnett, L.
Oklahoma State University, Stillwater, OK, United States
Klein, K., and Al Dushaishi, M. F.
Oklahoma State University, Stillwater, OK, United States
Nygaard, R.
University of Oklahoma, Norman, OK, United States
Hareland, G.
Oklahoma State University, Stillwater, OK, United States

This paper was prepared for presentation at the 55th US Rock Mechanics/Geomechanics Symposium held in Houston, Texas, USA, 20-23 June 2021. This paper was selected for presentation at the symposium by an ARMA Technical Program Committee based on a technical and critical review of the paper by a minimum of two technical reviewers. The material, as presented, does not necessarily reflect any position of ARMA, its officers, or members. Electronic reproduction, distribution, or storage of any part of this paper for commercial purposes without the written consent of ARMA is prohibited. Permission to reproduce in print is restricted to an abstract of not more than 200 words;

ABSTRACT: One challenge that hinders efficient drilling and causes downhole tool failures is severe drillstring vibrations. The objective of this paper is to identify the root cause of drillstring vibrations in deep geothermal wells and investigate their effect on drilling performance using data analytics and vibration modeling. A near-bit sub was utilized to collect vibration data, where the burst data was used to obtain the drillstring torsional natural frequency. The data showed that the highest lateral acceleration and stick-slip severities (SSS) occur at the higher mechanical specific energy (MSE) range, while the low vibration levels were encountered in the optimum range of the MSE curve. The elevated SSS levels consistently occur at the low to mid-range of applied RPM and the highest sonic velocity. Additionally, the lateral acceleration levels are higher at the low to mid-range of the applied RPM. The effect of drillstring vibration on drilling performance was recognized by the presented MSE analysis.

1. OVERVIEW

One of the key factors in optimizing the drilling process is maximizing ROP. Generally, operators attempt to do this by adjusting the weight on bit (WOB) and rotations per minute (RPM) while drilling. However, there are many reasons including but not limited to: bit type, rock type, fluid type, and rig capabilities, that can dramatically affect the drilling process, i.e. may increase ROP but drastically reduce the bit and/or bottomhole assembly (BHA) life. Drillstring vibrations can be categorized into axial, torsional, and lateral modes (Figure 1). Axial vibrations generally result in a phenomenon called bit-bouncing, which can cause significant damage to the PDC cutters and bit as a whole (Ashley et al., 2001). This is more prevalent in vertical sections, where the axial vibration modes tend to disperse themselves as inclination builds. Torsional vibrations tend to manifest as stick-slip. This is where the torque on the bit, due to the contact friction with the rock, causes the bit to momentarily stick until the buildup torque above the bit overcomes the frictional forces and breaks the bit free, i.e. slip. This phenomenon results in temporary excessive rotational speed of the bit, which can potentially over-torque the BHA connections, or potentially cause drillstring twist-offs (Ashley et al., 2001). Lateral vibrations occur when the rotation of the BHA is eccentric, causing side impact with the wellbore.

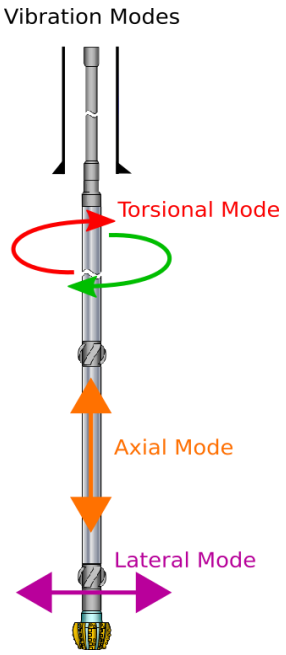

Fig. 1. Drillstring vibration modes.

Drillstring vibrations can be measured at the surface or downhole. At the surface, rigs are outfitted with sensors in the top drive and drawworks that will measure parameters such as surface RPM's, torque, and the applied WOB. Downhole tools such as measurement/logging while drilling (M/LWD) tools are equipped with a suite of sensors that, among other measurements, can measure vibration magnitude. These types of measurements can provide data in real time, as well as more precise, i.e. higher resolution, in memory mode.

Torsional vibrations, mainly stick-slip, are an extensively studied mode of drillstring vibrations. Generally, reducing the WOB for a given RPM or increasing the RPM for a given WOB will decrease the stick-slip severity (Richard et al., 2002). However, that's not always the case due to other factors such as BHA and bit designs, the formation being drilled, and the coupling between other vibration modes. PDC bits are prone to stick-slip vibrations which could lead to bit damage (Ledgerwood et al. 2013). Using numerical methods, Makkar et al. (2014) simulations suggest that as the drill bit transitions to unstable drilling, the lateral acceleration increases as well as the mechanical specific energy (MSE).

Traditionally, drillstring vibrations have been known to cause reduced ROP or bit/BHA damage, however an increase in ROP due to axial vibrations has been suggested (Babatunde et al., 2011). While it has been shown that the resultant vibrations have negative effects on the drill bit and BHA life, there is little information available that shows how drillstring vibrations affect ROP, and thus a strong correlation has yet to be determined.

The scope of this paper is to investigate the effect of drillstring vibration on ROP from data gathered during a field study. The data contains lateral accelerations and rotational speeds from downhole measurement systems used for two different bit runs. The vibration data was used to extract the natural torsional frequency of the drillstring. To verify the natural frequency of the drillstring, a finite element model is used. This model is based on the finite strain formulation, which can determine the natural frequencies of a given drillstring and BHA configuration.

2. FIELD DATA OVERVIEW

The well is located in the Chocolate Mountains Aerial Gunnery Range (CMAGR) in southern California, where the vertical well was drilled to 3020 ft (Raymond et al., 2012). Data collection included surface rig parameters, vibration-monitoring, BHA memory tools, and well logging measurements. The section of interest, in this work, is the drilled interval between 1345 ft to 2643 ft, where two different bits were used for the same size hole. The first bit, Bit 1, was an 8½ inch PDC with eight blades, eight nozzles, and was equipped with a torque control component, i.e. arrestors, that prevent the extreme depth of cut (Figure 2). Bit 1 drilled from 1345 feet to 2070 feet for total penetration of 725 feet. The second bit, Bit 2, was also an 8½ inch PDC with seven blades, seven nozzles, and no arrestors. Bit 2 drilled from 2070 feet to 2643 feet for a total drilling distance of 573 feet (Figure 2).

Fig. 2. Bit 1 (Left), Bit #2 (Right).

The BHA components used for both bit runs are similar with minor adjustment of stabilizer position for Bit 2 BHA. Table 1 shows the components of the two BHAs and each component dimension.

Table 1. Bit1 and Bit 2 BHA components

Comp.	OD (mm)	ID (mm)	Length (m)	
			BHA 1	BHA 2
DC	158.75	71.37	68.38	--
DC	158.75	71.37	53.72	60.16
Stab	215.90	63.50	1.30	--
DC	158.75	71.37	8.36	53.72
Stab	215.90	63.50	1.30	1.30
DC	158.75	71.37	8.45	8.36
Stab	215.90	63.50	1.15	1.30
DC	158.75	71.37	--	8.45
Bit Sub	165.10	50.80	0.91	0.91
BB Sub	165.10	38.10	0.46	0.46
Bit	215.90	50.80	0.30	0.30

The downhole vibration measurements were measured using the Black Box downhole measurement sub (Schen et al., 2005), which measures the downhole rotational speed, lateral and centripetal accelerations located in Table 1 just above the bit (i.e. BB Sub). The downhole rotational speed is computed by the Black Box plugs using the measured *x*, *y*, and *z* accelerations. The measurement sub provides data at two different sample rates: slow, and fast, i.e. burst data. The slow sample rate records a sample every 2.56 seconds throughout the bit run. The fast rate was set to record 400 samples per second for a period of 10 seconds, which was triggered every 5 minutes. The configurations of the downhole measurement sub consisted of two plugs that were staggered so a fast data set would be available every 2.5 minutes. For identification purposes, Bit 1 BHA consisted

of plug #762 and #789, and Bit 2 BHA consisted of plug #744 and #754.

The drilling parameter and logging data consisted of time-based and depth-based measurements with varying measurement frequencies, which requires synchronization. The data synchronizing consisted of aligning the time-based and depth-based data of the surface measurement system, logging, and downhole memory measurements. The process started with first re-sampling the rig parameter data and downhole data over a one-minute interval. The one-minute interval was chosen to reduce the large data size while still providing sufficient data quality. Next, the nondrilling data and outliers were filtered to aid in the analysis. The daily drilling report and reported drilling parameters were used as a base for filtering the data. As part of the filtering data were excluded when the surface rotational speed was less than 50 RPM, or the rate of penetrations were greater than 100 feet per hour or less than 5 feet per hour. After resampling and filtering the data, the RPM values for each data set were normalized and manually shifted in time to match the rig parameter data with the slow memory downhole data. After synchronizing the vibration data, i.e. time-based data, with the drilling depth-based data, the logging data were linearly interpreted based on the drilling depth. This procedure provides log files that contain drilling, vibration, and logging data that are used to evaluate the drilling process.

The mechanical specific energy (MSE), developed by Teale (1965), is a useful indicator for measuring the drilling efficiency, which has been adopted for this analysis. The MSE can be calculated in psi, based on the drilling parameters according to:

$$MSE = \frac{480 \times T \times RPM}{{D_b}^2 \times ROP} + \frac{4 \times WOB}{\pi \times {D_b}^2} \qquad (1)$$

Where T is torque measured in ft.lb, D_b is the drill bit diameter in inches, ROP is the rate of penetration in ft/hr., and the weight on bit (WOB) is measured in lbf.

The logging data, specifically the sonic travel time, can be used to obtain an estimate of the unconfined rock strength (UCS). For this analysis, the correlation of Oniya (1988) was adopted to calculate the UCS in psi based on the sound travel time Δt_c in μs/ft as shown in Eq. (2).

$$UCS = 1000 \times \left(\frac{1}{5.15 \times 10^{-5}(\Delta t_c - 23.87)^2} + 2\right) \qquad (2)$$

Stick-slip severity (SSS) indicator is used to measure the bit rotational speed with respect to the applied surface speed over a period of time. The SSS indicator in this analysis was calculated over a one-minute interval according to Eq. (3), where ΔRPM_D stands for the difference between the maximum and the minimum downhole rotational speeds measured over one period and RPMs is applied surface rotational speed.

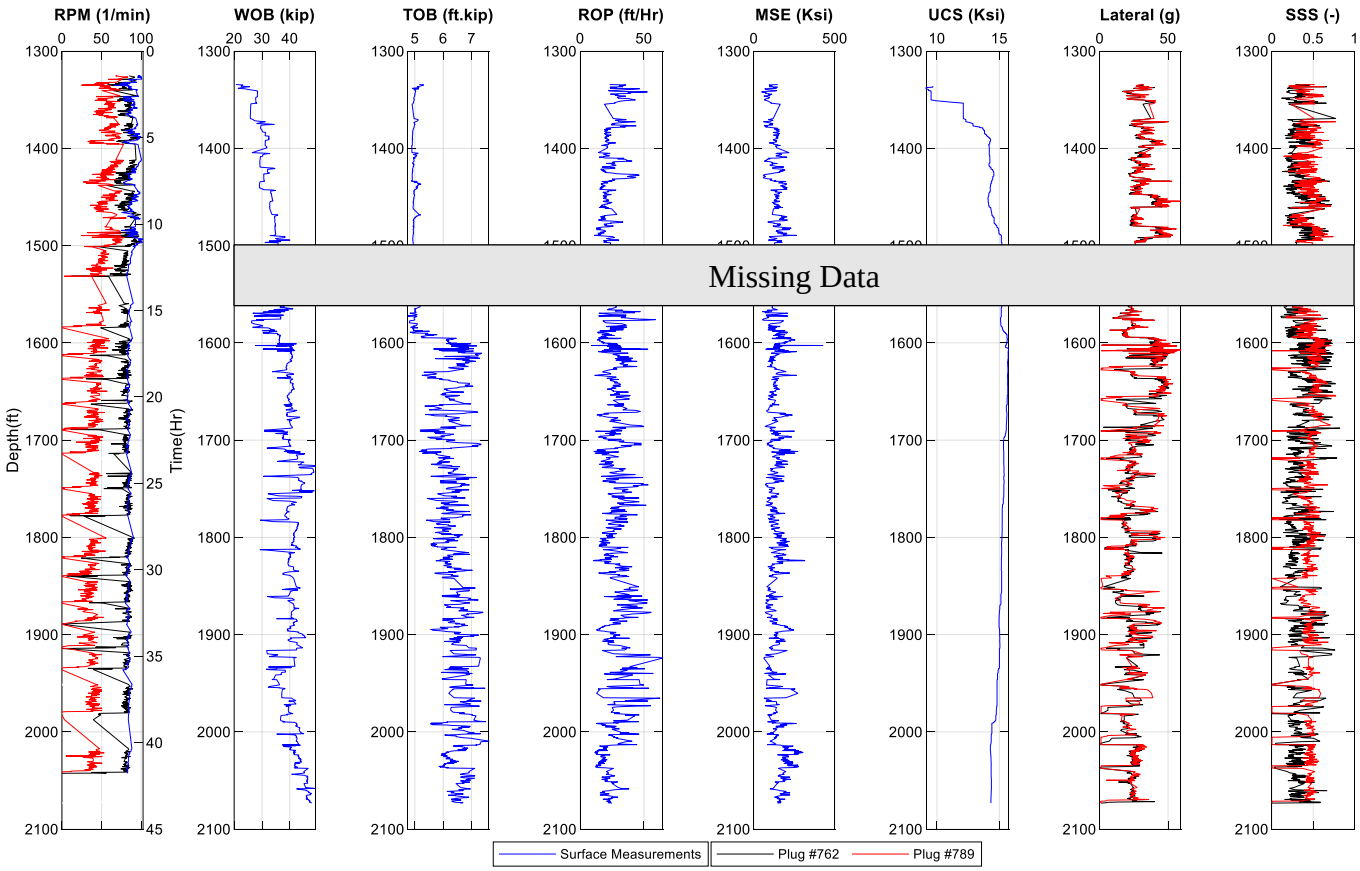

Fig. 3. Bit 1 synchronized well log.

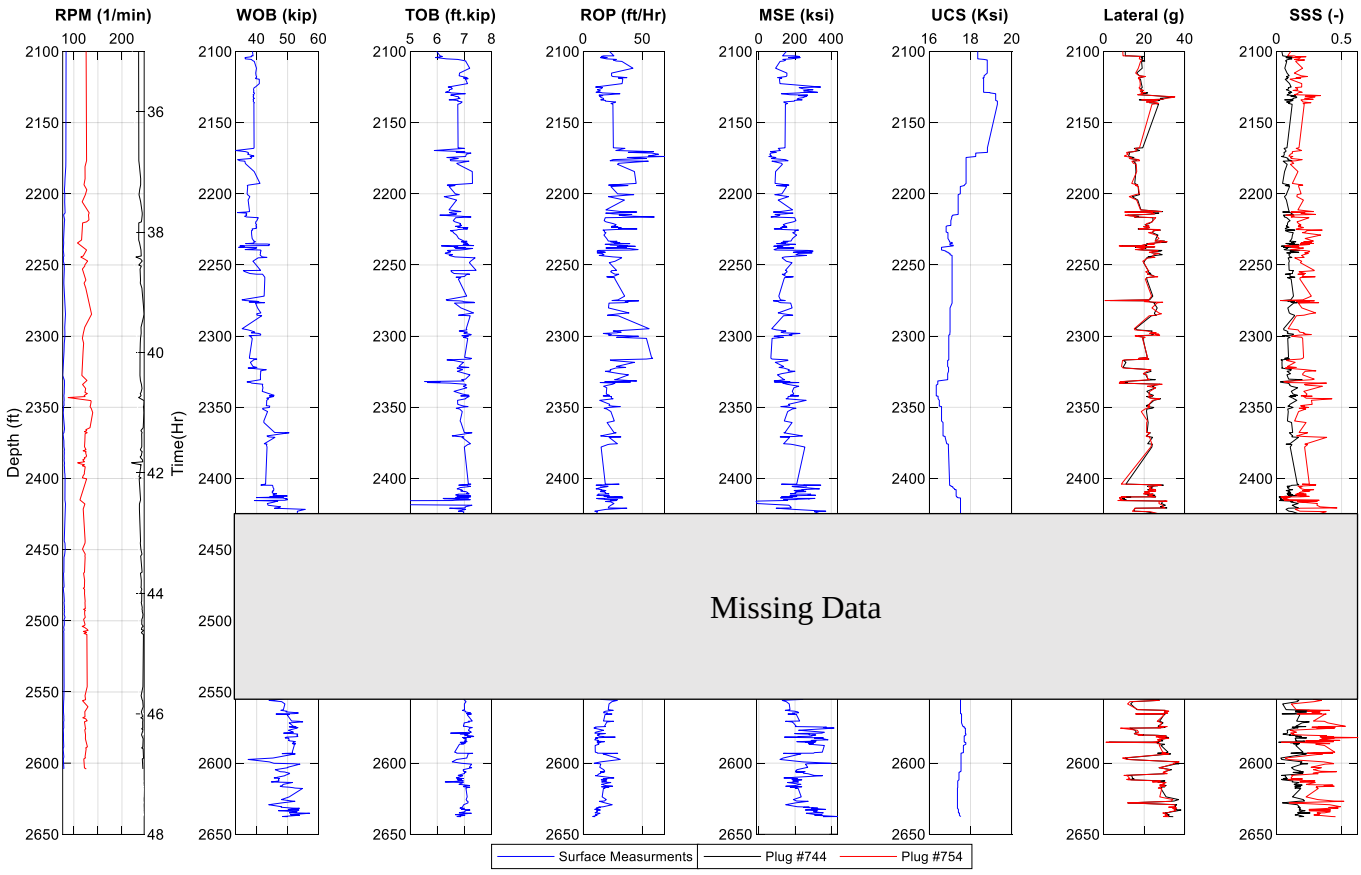

Fig. 4. Bit 2 synchronized well log.

$$SSS = \frac{\Delta \mathrm{RPM}_D}{2 \times RPM_S} \quad (3)$$

Based on the synchronized analysis, a detailed well-log is created for Bit 1 and Bit 2, as shown in Figure 3 and Figure 4, respectively. The well-log figures consist of the downhole RPM, WOB, torque on bit (TOB), ROP, lateral acceleration, and the calculated MSE and the SSS indicator.

For Bit 1, the rotational speed anomalies between Plug #762 and #789 are apparent in the RPM log. Between 1600 and 1700 feet, higher concentrations of elevated events of both stick-slip and lateral acceleration can be seen, where the UCS value is above 15 ksi. For Bit 2, the highest values of maximum lateral accelerations and stick-slip severity were encountered at the end of the bit run below 2550 ft. From the vibrations point of view, the lateral acceleration levels and SSS of Bit 1 are higher when compared to Bit 2. It is important to note that the SSS for both bits did not reach severe levels.

3. DRILLSTRING NATURAL FREQUENCY DETERMINATION

3.1. Field Data Frequency Analysis

With the time domain data recorded by the Black Box, it is possible to analyze the frequency spectrum using fast Fourier transform (FFT) analysis with a sampling frequency of 400 Hz. The purpose for examining the data as a function of frequency is the capability of determining the dominant natural and forced frequencies of the system. To determine the natural frequencies of the system, an FFT analysis was performed on the frequency spectra of the rotational speed. Before analysis could start, the rotational speeds were normalized, removing the DC component of the signal. To determine the drillstring natural frequency, it was important to identify the data set for non-drilling events. The purpose for only analyzing non-drilling data sets was the presumption that there will be fewer external forces and friction in the system. Therefore, it was concluded that examining only non-drilling data sets would display a more distinct natural frequency. This was performed with the assumption that the results would not be overwhelmed by the forced frequencies created during the drilling process. All 4 plugs were analyzed to determine the natural frequency of the system. Figure 5 shows the amplitude spectrums for all 4 plugs after averaging the data from all burst files of 10 s identified as non-drilling. It is clear from this figure that 3.1 Hz is the dominant frequency.

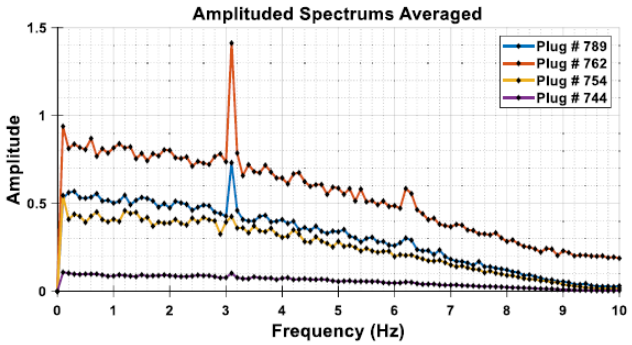

Fig. 5. Averaged Amplitude Spectrum for all plugs.

To verify that 3.1 Hz is an accurate fit, a 3.1 Hz sine wave was overlaid on a Black Box fast file, where non-drilling occurred, from Plug #789 in Figure 6. By visually inspecting Figure 6 the wavelength is comparable between the two wave sets.

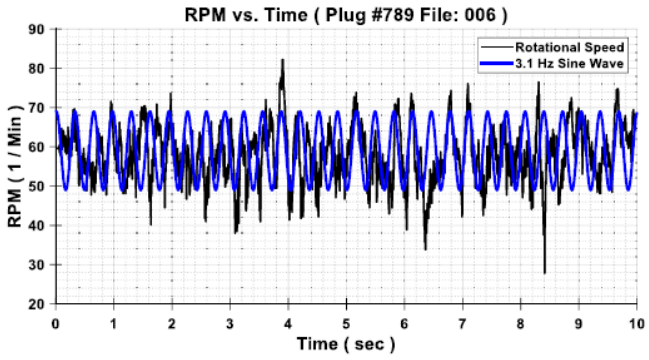

Fig. 6. A sine wave of 3.1 Hz Overlaid with Plug#789 measurements.

3.2. Model-Based Frequency Determination

A finite element model, based on a continuous model approach, was used to calculate the natural frequencies of the drillstring axial, lateral, and torsional modes. The model assumed that the shear forces due to bending are negligible and uses the finite element method to solve the equation of motion (Al Dushaishi et al., 2017). For the boundary conditions, the drillstring was assumed to be fixed in the axial and lateral motion at the rotary table and a constant axial rotational speed is imposed. At the bit, the lateral displacement was assumed fixed, and the axial displacement is constrained around the static equilibrium position allowing it to vibrate. The BHA components (Table 1) were used to obtain the drillstring natural frequencies. Table 2 shows obtained first five modes of axial, lateral, and torsional drillstring frequencies for DS 1 and DS 2 at the total drilled depth, which correspond to Bit 1 and Bit 2, respectively.

Table 2. Calculated drillstring frequencies.

Mode No.	Axial (Hz)		Torsional (Hz)		Lateral (Hz)	
	DS 1	DS 2	DS 1	DS 2	DS 1	DS 2
1	1.19	1.02	0.65	0.57	0.03	0.05
2	5.59	4.21	3.44	2.57	0.06	0.09
3	10.72	7.95	6.66	4.92	0.10	0.15
4	15.64	11.79	9.78	7.32	0.12	0.16
5	18.40	15.60	11.37	9.71	0.14	0.19

The measured drillstring frequency of 3.1 Hz corresponds to the calculated second torsional mode of DS1 and DS 2 (Table 2). It can be observed that the difference between the measured and calculated frequencies is 0.3 Hz and 0.5 Hz for DS 1 and DS 2, respectively.

4. DATA ANALYTICS OF DRILLSTRING VIBRATIONS FIELD DATA

Stick-slip and lateral acceleration events for both bit runs are summarized in Table 3, which shows the frequency of the severity levels events of stick-slip and lateral accelerations throughout the bit runs. For Bit 1 plug #762, the calculated stick-slip severity showed that the maximum observed severity was 0.82, which falls under the moderate category. Over 80% of the observed stick-slip severity was considered in the low range for Bit 1. It can be observed for Bit 1 that the severe lateral accelerations represent around 26% of the drilling events, while the majority of the drilling events fall in the moderate levels. The stick-slip severity data for Bit 2, Plug #754, indicates that most of the drilling events fall under the low severity range. The lateral acceleration for Bit 2 was mainly concentrated in the moderate range of severity.

Comparing the two-bit runs, Bit 1 showed a higher occurrence of severe lateral vibration events when compared to Bit 2. The slight change in the bit and BHA designs could have a role in this behavior. The BHA for Bit 1 consisted of a near-bit stabilizer, while for Bit 2 the stabilizer was placed approximately 30 ft above the bit (Table 1).

Table 3. Statistics of stick-slip and lateral acceleration severities.

Stick-Slip Severity Level					
Bit 1			*Bit 2*		
Range (-)	No. Cases	Severity Level	Range (-)	No. Cases	Severity Level
0.0-0.5	1168	Low	0.0-0.5	464	Low
0.5-1.0	223	Moderate	0.5-1.0	4	Moderate
1+	0	Severe	1+	0	Severe
Maximum Lateral Severity Level					
Bit 1			*Bit 2*		

Range (g's)	No. Cases	Severity Level	Range (g's)	No. Cases	Severity Level
0-15	225	Normal	0-15	156	Normal
15-35	1827	Moderate	15-35	759	Moderate
35+	730	Severe	35+	21	Severe

To get more insight into the vibration effect on drilling performance, the MSE was used as the performance indicator. Figure 7 (a) and (b) show the MSE versus ROP for different intervals of WOB and sonic travel time with lateral RMS accelerations as the gradient color for Bit 1 plug #762 and Bit 2 plug # 754, respectively.

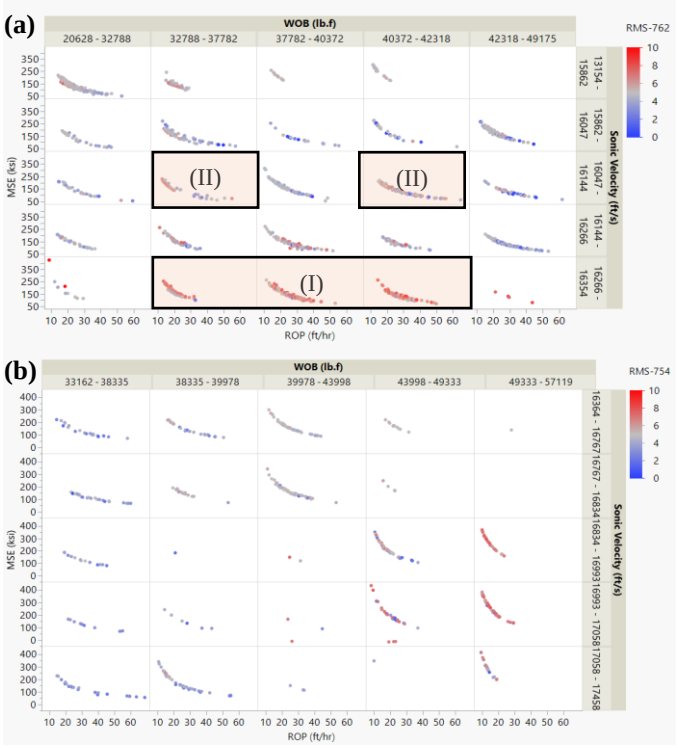

Fig. 7. MSE Vs. ROP with respect to lateral RMS acceleration binned with respect to WOB and Sonic Velocity for (a) Bit 1 (b) Bit 2.

For Bit 1 (Figure 7-a), it can be observed that the highest lateral accelerations are mainly manifested in the high sonic travel time region as shown in region-I, where it can be seen that the density of the elevated lateral accelerations increases as the WOB increases. Region II in Figure 7-a shows a noticeable relationship between the lateral acceleration levels and MSE, where the elevated lateral accelerations are seen in the upper MSE curve, i.e. suboptimal region. However, this relationship between MSE and lateral RMS is not apparent in the high sonic travel time regions. For Bit 2 (Figure 7-b), the density of elevated RMS accelerations tends to slightly increase as WOB increases. Most of the elevated lateral RMS accelerations are seen in the suboptimal regions in the MSE curves, while the lowest accelerations can be seen at the lowest applied WOB range.

With respect to stick-slip severity, Figures 8 (a) and (b) show MSE versus ROP for different intervals of WOB and sonic travel time with stick-slip severity as the gradient color for Bit 1 plug #762 and Bit 2 plug # 754, respectively. For Bit 1, the highest density of high stick-slip severity is located in the middle ranges of WOB and the high sonic velocity region, i.e. harder rock (Figure 8-a). While Bit 2 Figure 8-b, the higher density of stick-slip severity is concentrated in the high range of WOB. Overall, the data showed no clear relationship between stick-slip severity and MSE for both bit runs.

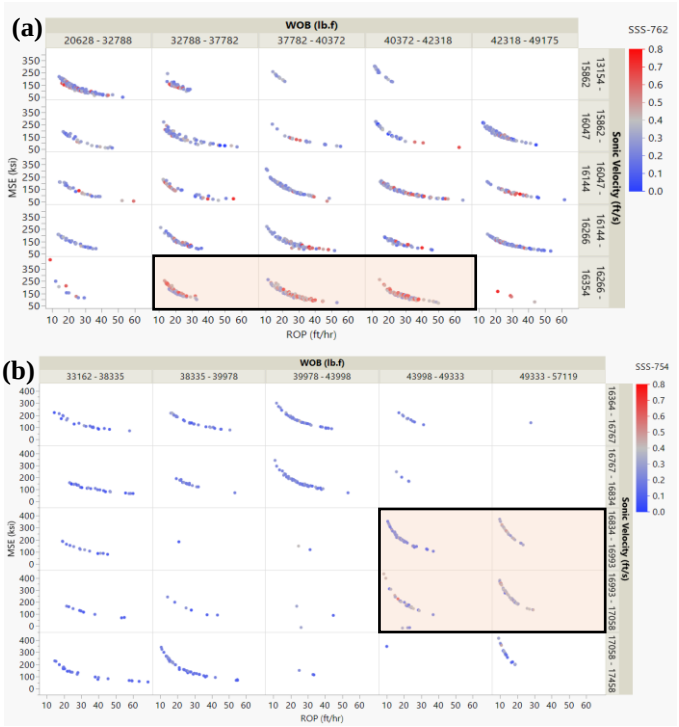

Fig. 8. MSE Vs. ROP with respect to stick-slip severity binned with respect to WOB and Sonic Velocity for (a) Bit 1 (b) Bit 2.

Comparing the drillstring vibrations for both bits, Figure 9 shows the MSE curve with respect to (a) the lateral RMS acceleration and (b) the stick-slip severity. The MSE curves, with respect to the lateral RMS accelerations (Figure 9-a), show that the elevated RMS accelerations mainly occur in the inefficient region of the MSE curve.

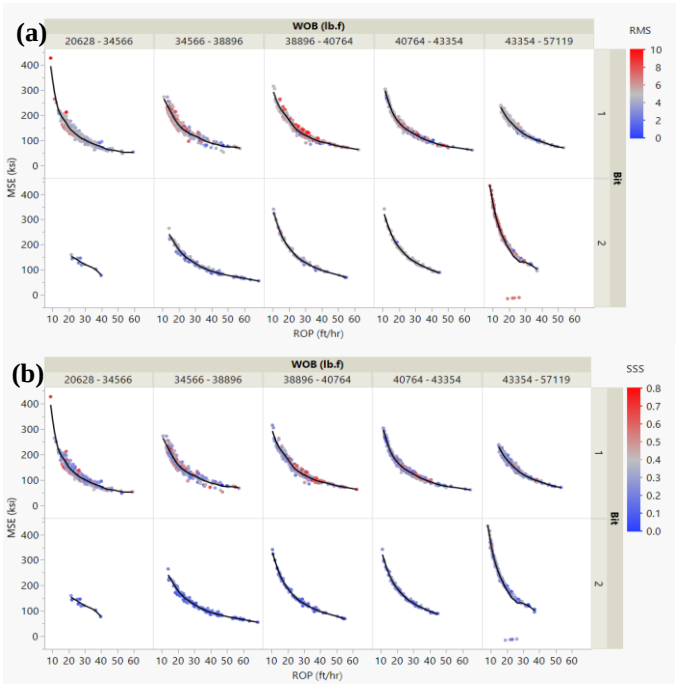

Fig. 9. MSE Vs. ROP for Bit 1 and Bit 2 with respect to (a) lateral RMS acceleration (b) stick-slip severity binned with respect to WOB.

For Bit 2 (Figure 9-b), the highest density of elevated RMS accelerations was encountered at the high region of applied WOB, where the MSE curve indicates the least optimum drilling for the entire bit run. In terms of stick-slip severity, Bit 2 showed lower stick-slip severity compared to Bit 1. The concentration of elevated stick-slip severity for Bit 1 is mainly noticed in the middle range of the applied WOB. For Bit 2, the highest stick-slip severity was reached in the high WOB region (Figure 9-b) following the lateral RMS acceleration behavior shown in Figure 8-b.

5. CONCLUSION

Drillstring vibration analysis in a hard rock geothermal well was presented in this paper. The analysis consisted of analyzing the torsional and lateral drillstring vibrations and their effect on drilling performance. Overall, the torsional vibration data showed an insignificant relationship with ROP, which could be due to the lack of severe stick-slip events and generally low ROP throughout the bit runs. The elevated stick-slip severity was mainly encountered in the highest sonic velocity region for Bit 1, and in the moderate to high sonic velocity region for Bit 2. Bit 2 has high stick-slip severity late in the bit run that may be due to the more aggressive torque nature of this bit that exceeded rig torque delivery capabilities; this resulted in frequent rig top drive stalls and may have contributed to cutting structure damage, deteriorated performance, and elevated vibrations as it approached final depth.

The FFT analysis of the downhole rotational speed revealed that the natural frequency of the drillstring was 3.1 Hz, which closely matches the mode of the calculated frequency using the finite element model. The determination of the drillstring natural frequency enables the operator to avoid operating the drillstring at its natural frequency to mitigate the likelihood of damaging vibrations.

The field data analysis indicated that increasing WOB is directly and proportionally related to the lateral acceleration levels. It was also found that there is a noticeable relationship between lateral acceleration levels and MSE, where the elevated lateral RMS acceleration is mainly seen in the upper MSE curve, i.e. inefficient region.

Comparing the vibration data for both bits, Bit 1 showed noticeably higher values of both stick-slip and lateral accelerations. While the drilling parameters and rock formations affect the vibration levels, the BHA used can also play a major role. The BHA of Bit 1 consisted of an additional stabilizer with a total of three stabilizers when compared to Bit 2 BHA with two stabilizers. The difference in cutting structures between Bit 1 and Bit 2 likely contributed to the differences in vibration levels and overall response, however, the evaluation of that difference is beyond the scope of this paper. Further research will include controlled laboratory experiments at Sandia National Laboratories to further quantify the effects of drillstring vibrations on ROP.

ACKNOWLEDGEMENT

This material is based upon work supported by the U.S. Department of Energy, Office of Energy Efficiency & Renewable Energy, under Award Number EE0008603. We also wish to acknowledge the Navy Geothermal Program Office for permission to use the field data. Lastly, we would like to acknowledge David Raymond and Sandia National Laboratories for their help and support with the field study.

REFERENCES

Al Dushaishi, M., Nygaard, R. and Stutts, D. 2017. An Analysis of Common Drill Stem Vibration Models. Journal of Energy Resources Technology, Vol. 140(1), https://doi.org/10.1115/1.4037682.

Ashley, D. K., McNary, X. M., and Tomlinson, J. C. 2001. Extending BHA Life with Multi-Axis Vibration Measurements. Presented at the SPE/IADC Drilling Conference, 27 February – 1 March, Amsterdam, Netherlands. https://doi.org/10.2118/67696-MS.

Babatunde, Y., Butt, S., Molgaard, J., and Arvani, F. 2011. Investigation of the Effects of Vibration Frequency on

Rotary Drilling Penetration Rate Using Diamond Drag Bit. Presented at the 45th US Rock Mechanics/Geomachanics Symposium, 26-29 June, San Francisco, CA.

Bavadiya, V., Alsaihati, Z., Ahmed, R., and Gustafson, K. 2017. Experimental Investigation of the Effects of Rotational Speed and Weight on Bit on Drillstring Vibrations, Torque and Rate of Penetration. Presented at the International Petroleum Exhibition & Conference, 13-16 November, Abu Dhabi, UAE. https://doi.org/10.2118/188427-MS.

Christian, E. 2017. Identifying the Optimum Zone for Reducing Drill String Vibrations. Presented at the SPE Annual Technical Conference and Exhibition, 9-11 October, San Antonio, TX. https://doi.org/10.2118/189284-STU.

Ledgerwood III, L.W., Jain, J. R., Olivier, H. J., and Spencer, R. W. 2013. Downhole Measurement and Monitoring Lead to an Enhanced Understanding of Drilling Vibrations and Polycrystalline Diamond Compact Bit Damage. SPE Drill & Compl 28(3): 254–262. https://doi.org/10.2118/134488-PA.

Makkar, N., Sullivan, E., and Habernal, J. 2014. Coupling Between Lateral and Torsional Vibrations: A New Insight into PDC Bit Drilling Inefficiencies. Presented at the Offshore Technology Conference-Asia, Kuala Lumpur, Malaysia, March 25–28. https://doi.org/10.4043/25056-MS.

Onyia, E. C. 1988. Relationships Between Formation Strength, Drilling Strength, and Electric Log Properties. Presented at the SPE Annual Technical Conference and Exhibition, Houston, Texas. https://doi.org/10.2118/18166-MS.

Raymond, D., Knudsen, S., Blankenship, D., Bjornstad, S., Barbour, J., and Schen, A. 2012. PDC Bits Outperform Conventional Bit in Geothermal Drilling Project, GRC Resources Council Transactions, v.6, p.307-315.

Richard, T., Detournay, E., Fear, M., Miller, B., Clayton, R., and Matthews, O. 2002. Influence Of Bit-Rock Interaction On Stick-Slip Vibrations Of PDC Bits. Presented at the SPE Annual Technical Conference and Exhibition, San Antonio, Texas, September 29–October 2. https://doi.org/10.2118/77616-MS.

Schen, A., Snell, A., and Stanes, B. 2005. Optimization of Bit Drilling Performance Using a New Small Vibration Logging Tool. Presented at the SPE/IADC Drilling Conference, 23-25 February, Amsterdam, Netherlands. http://dx.doi.org/10.2118/92336-MS.

Teale, R. 1965. The Concept of Specific Energy in Rock Drilling. International Journal of Rock Mechanics, 2(1), pp. 57-73. https://doi.org/10.1016/0148-9062(65)90022-7.